MARY KAY O'CONNOR PROCESS SAFETY CENTER
TEXAS A&M ENGINEERING EXPERIMENT STATION

20th Annual International Symposium
October 24-26, 2017 • College Station, Texas

Oil Transportation in Pipelines with the Existence of Ice

Hongfei Xu*, E. Pereyra, E. Dellacase, and M.Volk,
McDougall School of Petroleum Engineering
The University of Tulsa
800 S Tucker Dr, Tulsa, OK 74104
* Presenter E-mail: hpx408@utulsa.edu

Abstract

When the ambient temperature is below freezing point, ice may form in the oil transportation pipelines, which can cause flow assurance issues, such as restricting flow path or even plugging the pipeline. Ice plugging was reported to delay the restart of the Poplar pipeline system gathering crude oil from Montana and North Dakota. [1] Ice may also pose threats to the Trans-Alyeska Pipeline System (TAPS). The declining throughput makes the oil get colder much faster. If oil temperature falls below the freezing point, ice forms and leads to flow assurance issues, such as coating critical valves, accumulating in the pipeline, and restricting flow. [2]

This paper investigates the fundamentals of ice formation in the pipeline and its effect on the transportation system. A 2-inch diameter carbon steel flow loop was instrumented to measure pressure, temperature, and differential pressure. The experimental results show that ice formation can restrict flow at the low sport in front of the flow meter, the inserted thermocouples, and the perforated plate. Annular ice deposition was found at the pipe wall. The morphology of the deposition is rime ice, indicating the deposition is due to small ice crystals sticking to the pipe surface. It was found that the formation of annular deposition requires a negative temperature gradient. The effect of water cuts and fluid properties on plugging tendency is discussed. The mechanisms for ice deposition along the pipe and plugging at the pipe components are proposed.

Introduction

Oil companies have taken aggressive measures to ensure continuity in oil supply to satisfy global energy needs, which led to the oil and gas exploration and production activities in harsh environments including extremely low temperatures. In 2008, the U.S. Geological Survey (USGS) estimated that the existing fields beyond the Arctic Circle account for 10% of the world's existing conventional resources. [3] Due to the low temperature conditions, water, even in trace amounts,

may form ice and lead to pipeline blockages and associated risks. Recently, ice formation and its associated risk threat due to declining throughputs in Trans-Alyeska Pipeline Systems(TAPS) has been determined, which leads to millions of dollars into ice formation research. [2]

Although ice may place potential threat to the transportation systems, very limited research was reported. Nevertheless, the study of hydrates provides insights that may be applied to the ice deposits. Traditionally, hydrate risks were avoided by maintaining the pipeline fluid temperature above the hydrate formation temperature, which requires large operational cost. [4] Instead, operational cost can be reduced by applying risk-control techniques, including the anti-agglomerant (AA) method [5][6] and the cold-flow technology without additional reagents, in which hydrate formation is permitted [7][8]. If risk-control techniques can be applied to ice in pipeline, the operational cost for pipelines can be reduced.

Ice formation was widely studied in meteorology, aviation, and the cooling industry. The findings from these studies have great value to the studies of ice formation in the oil transportation system. Highly supercooled water has been observed in cirrus and orographic waves, which is attributed to the small droplet size and lack of ice nuclei at the heights of these clouds. Rosenfeld and Woodley [9] reported that by maintaining the water droplet median volume diameter of 17 micron, most of the studied droplets remained liquid. However, the supercooled droplets impacting on aircraft wings transform into ice, which may stay on the wing surface. The added burden of the ice may lead to the crash of the aircraft. Thus, ice accretion on structures due to relative movement was studied by aviation industries. [10] It was reported that ice slurry is an excellent coolant. XXX studied the flowing behavior of ice slurry in tubes. [11]

The objectives of this study are to investigate the ice deposition and plugging issues in a liquid hydrocarbon and low water cut system. Three working fluids were used including kerosene (45^{o} API, 1.6 cp at 70 ^{o}F), a light crude oil (45^{o} API, 2% wax content, 11 cp at 70 ^{o}F), and a blend of the two oils. The effect of pipeline geometry was studied, including low spots, straight pipe section with an inserted rod, and straight pipe section with a perforated plate. The perforated plate is to mimic the protection screens implemented in TAPS pump stations. The protection screens keep the solids and trash out of the pump station to protect the pump and on-line instruments. In addition, the perforated plate has been applied to study jamming induced hydrate plugging issues in a pipeline. [12] This study shows the location where ice accumulation can occur, how long it takes to start this accumulation, and how long the ice accumulation turns into a plug.

Experimental Procedures and Materials

Flow Loop

In order to study ice deposition and evaluate its risks, a lab scale flow loop system was constructed in the University of Tulsa, as shown in Figure 1. [13] The experimental facility consists of four components, including a cooling system, a flow loop with a buffer tank, a control system, and a data acquisition system.

During the test, fluid was first charged into the buffer tank and then to the flow loop. A gear pump (CHEMSTEEL, SM946-M) was used to circulate the test fluid. Fluid can go through a

Coriolis mass flow meter (EMERSON, model number: CMF100M328NQBAF2ZZ) for flow rate measurements. A by-pass section was installed and applied when the flow meter was not required in the loop. After the Coriolis mass flow meter and its by-pass section, the fluid entered two cooling sections and then the test section. These three sections were jacked with 4-inch inner diameter carbon steel pipes. A chilled coolant mixed by glycol and water (50%-50%) was circulated inside the annulus of the jackets. The coolant temperature range can be between -10 ^{o}F and 120 ^{o}F, with a fluctuation of ±5 ^{o}F. The length of the test section is 31 inches. If a plate is installed, the plate locates at 18 inches from the test section entrance.

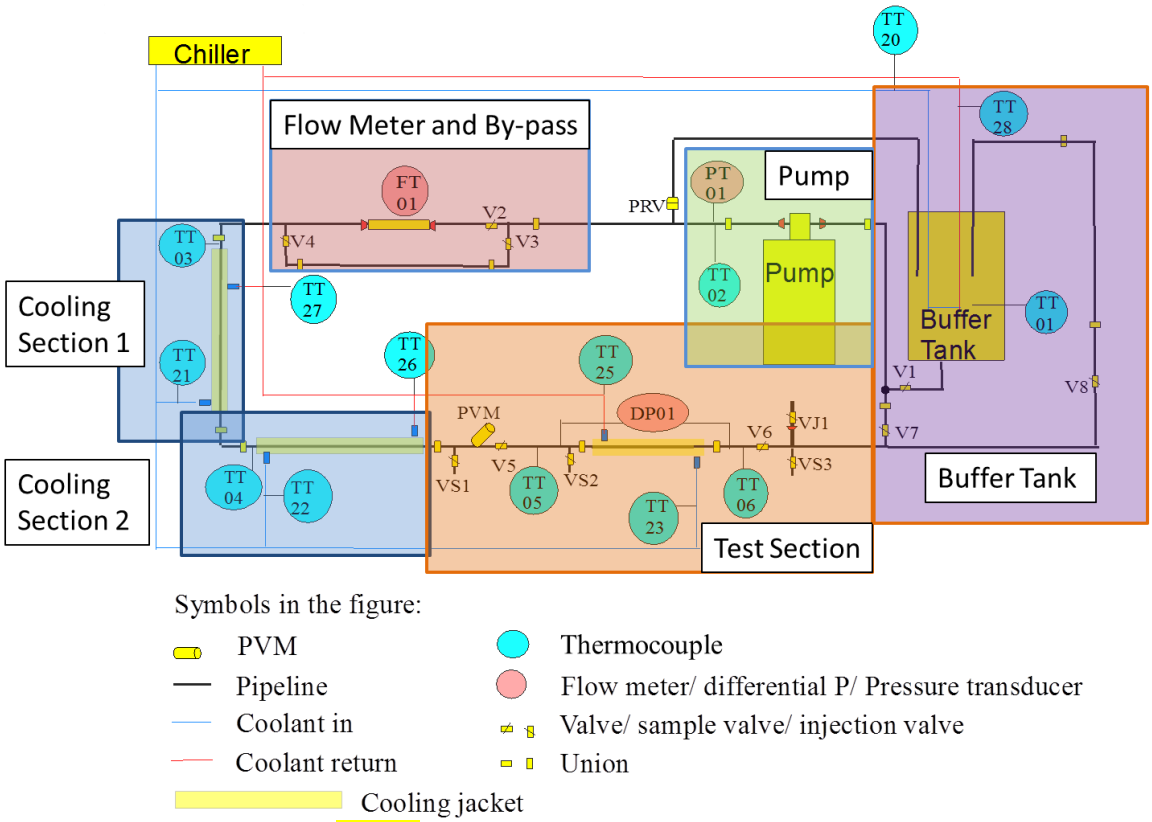

Figure 1: Schematic of the flow loop

During the test, fluid was first charged into the buffer tank and then to the flow loop. A gear pump (CHEMSTEEL, SM946-M) was used to circulate the test fluid. Fluid can go through a Coriolis mass flow meter (EMERSON, model number: CMF100M328NQBAF2ZZ) for flow rate measurements. A by-pass section was installed and applied when the flow meter was not required in the loop. After the Coriolis mass flow meter and its by-pass section, the fluid entered two cooling sections and then the test section. These three sections were jacked with 4-inch inner diameter carbon steel pipes. A chilled coolant mixed by glycol and water (50%-50%) was circulated inside the annulus of the jackets. The coolant temperature range can be between -10 ^{o}F and 120 ^{o}F, with a fluctuation of ±5 ^{o}F. The length of the test section is 31 inches. If a plate is installed, the plate locates at 18 inches from the test section entrance.

FactoryTalk (Rockwell Software®) was implemented as data acquisition system to record flow rate, pump differential pressure across the test section (labeled as DP), coolant temperatures, and

fluid temperatures inside the flow loop. Samples were taken from valves VS1 and VS3 for water cut and wax content analysis. Unions (carbon steel) were used to connect pipe sections, which makes it possible to take off pipe sections for examination, for example the test section. After isolation valves (V5 and V6) were turned off and the test section was drained using VS2, the test section can be taken out to examine ice deposition in the inner pipe.

Test Fluids

Three fluids were used in this study, CITGO low sulfur Kerosene, Oklahoma Sweet crude oil (OK Sweet), and a blend of the two oils. The kerosene has an API gravity of 45°. OK Swee has an API gravity of 45° and its wax content is 2%. The blend was made of 50 vol% kerosene and 50 vol% OK Sweet. The densities and viscosities of the three test fluids were measured using a Stabinger Viscometer (Anton Paar, SVMTM 3000). The results are shown in Figure 2

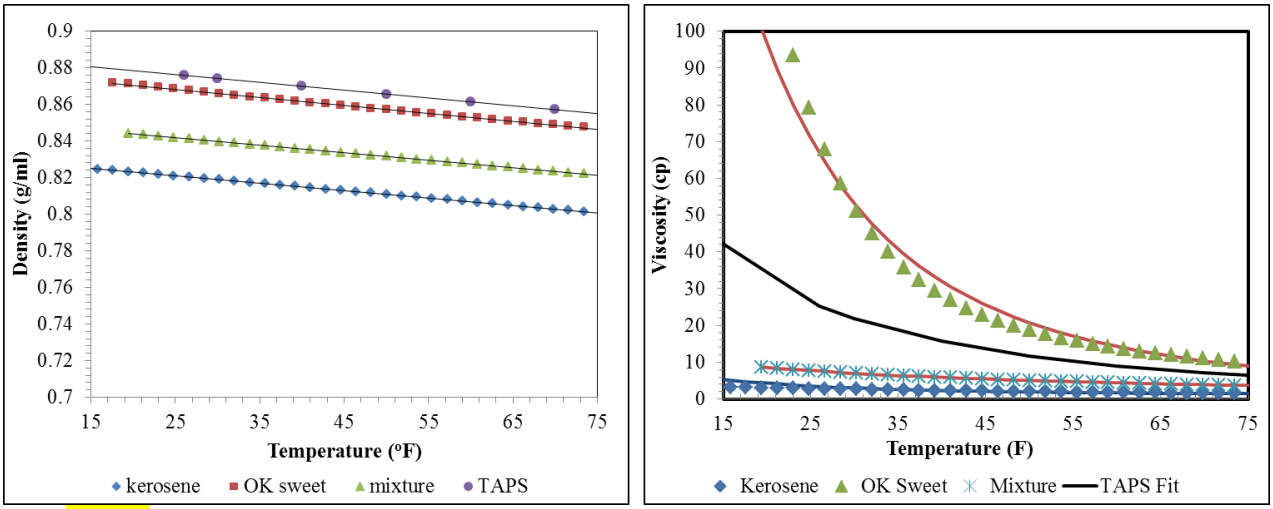

Figure 2: Densities and viscosities of kerosene, OK Sweet, mixture and TAPS crude oil

Test Matrix

Based on the research objectives and facility limitations, experimental matrix is planned, which is shown in Table 1.

Table 1: Experimental matrix.

Test #	Fluid	Test Section Geometry	Initial Water Cut (%)
1	Kerosene	No plate	1.297
2	Kerosene	No Plate	1.302
4	Kerosene	Plate	1.452
6	OK Sweet	Plate	1.455
7	Blend	Plate	1.901
8	Blend	Plate	1.323
10	Blend	Plate	0.693
11	Blend	Plate	0.802

Test 1, 2, and 3 used a straight pipe without plate at the test section. In Test 1, the flow meter was connected with the flow loop. In front of the flow meter, an uphill section was concerned to be one location that ice can accumulate. The test section in Test 4 applied the perforated plate. Test fluid of Test 1, 2, 3 and 4 are Kerosene. OK Sweet was used as the test fluid in Test 6. Test 7, 8, 10 and 11 used the blend. The effect of water cut was obtained by comparing Test 7,8, and 11. In Test 10, the test section was opened four times to observe the plugging process at the plate. The flow rate of all tests was maintained at 12 GPM.

Experimental Results

Plugging Pipe Components

Ice accumulation was found at the uphill section in front of the flow meter, the inserted thermocouple, and the perforated plate. Plugging due to ice accumulation occurred for Test 4, 6, 7 and 8, but not for Test 10 and Test 11.

Ice deposition at the low spot was identified by comparing the experimental data from Test 1 and Test 2. Figure 3 shows the experimental data comparison between Test 1 and Test 2. In test 1, ice particles may separate and accumulate at the uphill sections when the test fluid passes through the flow meter. The accumulated ice particles blocked the flow path, which was shown by comparing the pump outlet pressure in Test 1 and Test 2

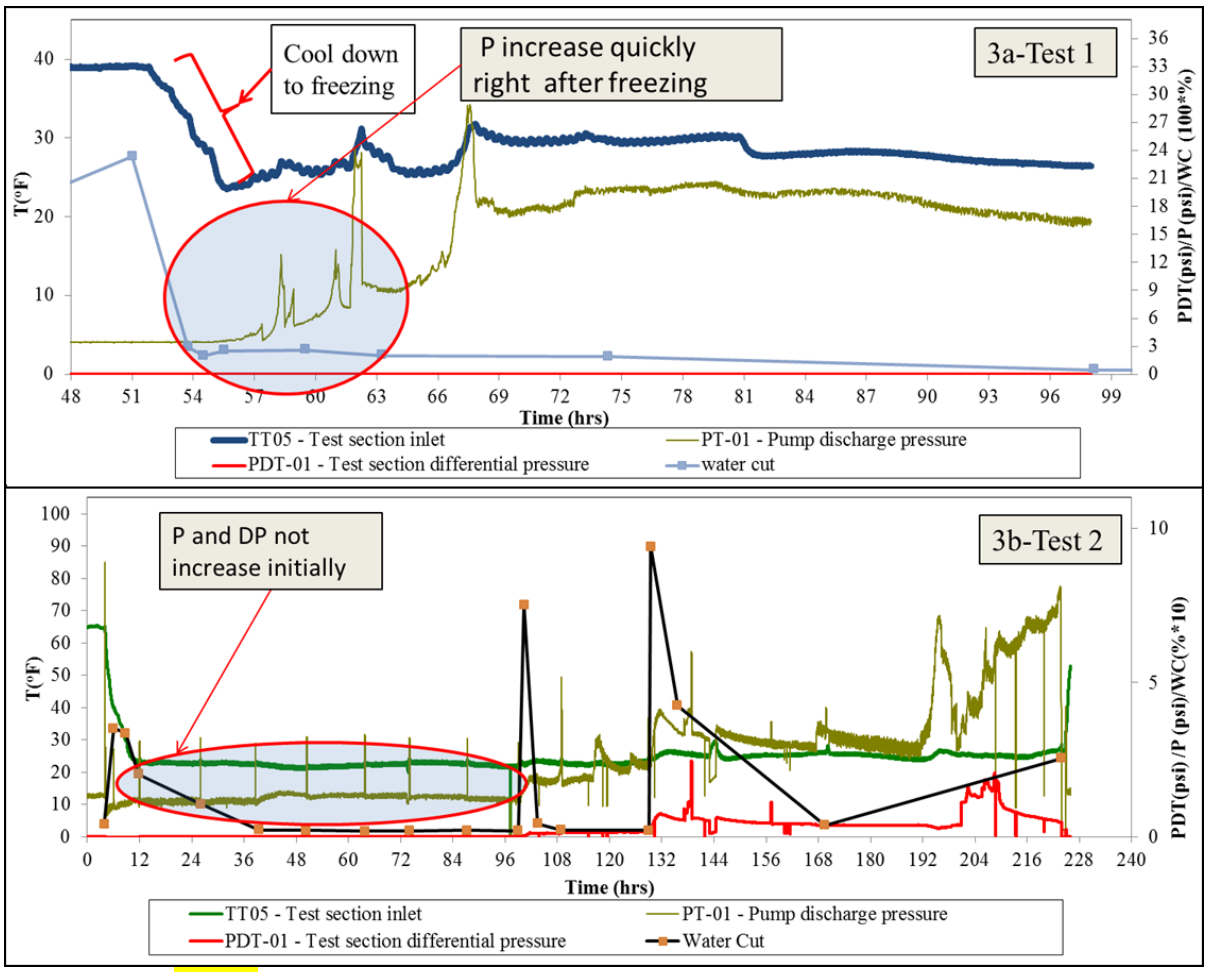

Figure 3: Experimental data comparison between Test 1 and Test 2

The flow meter in the flow loop is installed vertically. Ice accumulated in front of the flow meter, where ice particles need to climb up to go through the flow meter. The flow meter was in line in Test 1. The pump outlet pressure (P) increased right after the fluid temperature reached the freezing point, while the differential pressure (DP) across the test section remained almost constant. This indicated the flow path was restricted not in the test section, but other sections. Along the flow loop, the only spot that can have the potential to restrict flow is at the low spot in front of the flow meter. In contrast, in Test 2, the by-pass section was applied and the flow meter was offline. After the fluid temperature decreased below the freezing point, pump outlet pressure did not change until the differential pressure started to increase at 96 hours, which indicated the flow path was restricted in the test section. In Test 2, the perforated plate was not installed. After the test section was disassembled, it was found that ice accumulated at the inserted thermocouple, which blocked the flow and led to the increase of differential pressure. Figure 4 shows the ice plugs at the thermocouple.

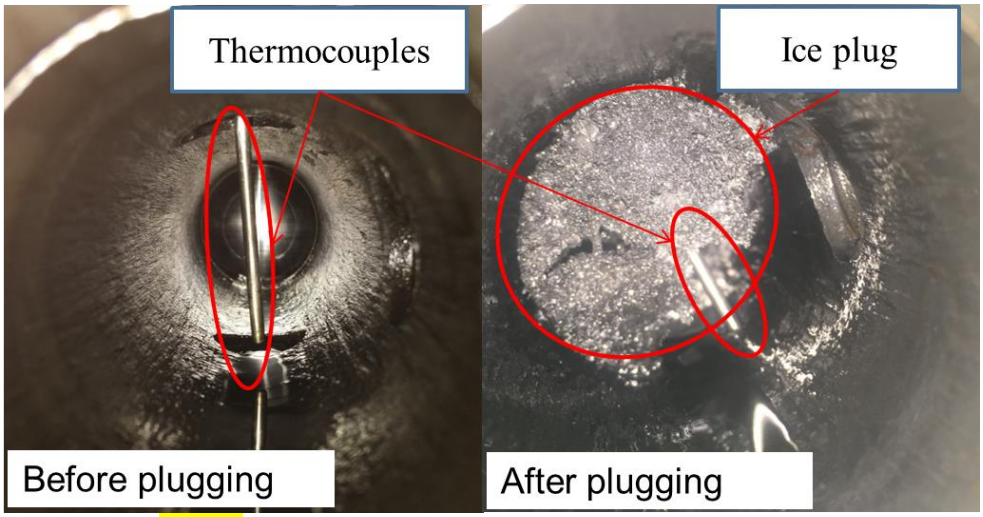

Figure 4: Ice plug at the inserted thermocouple (TT05)

Plugging was also observed on the perforated plate in the test section. Figure 5 shows the ice plugs at the perforated plate. In the kerosene test (Test 4), the plate was not fully covered by ice, but the pores on the plate were all plugged. In the OK Sweet test (Test 6), the plate was fully covered by a transparent glaze ice. In Test 7, the plate was fully covered by rime ice. In Test 8, the plate is not fully covered. The pores in Test 7 and 8 are all plugged. No complete plug was shown in Test 11.

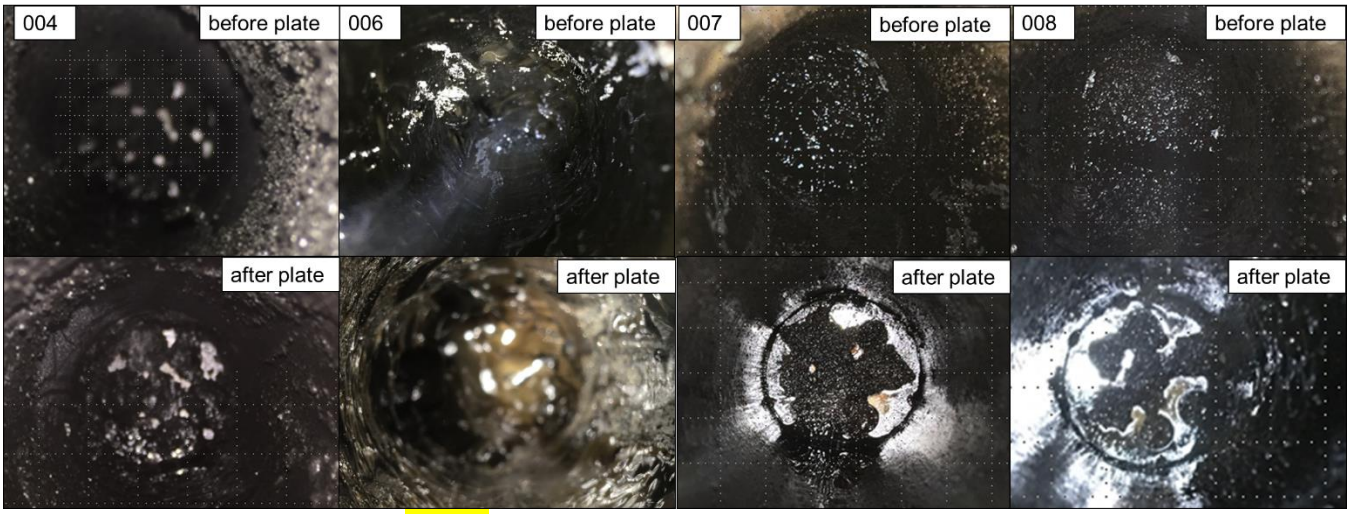

Figure 5: Ice plugs at perforated plate

The perforated plate is used to simulate the protection screens in TAPS, which are used to prevent the solids in the pipeline entering the pump station. Thus, in addition to observe the morphology of the ice plugs at the plate, it is important to obtain the information of when the ice accumulation starts and how long it takes to plug the plate.

The plugging tendency test for the three test fluids are compared, which was shown in Figure 6. For the test using kerosene, differential pressure across the test section started to increase 4 hours after the fluid temperature reaches 32 ^{o}F. A complete plug at the plate is defined to form

after the pump outlet pressure reaches 40 psi. Although differential pressure continued to increase, a complete plug was not observed during the entire experiment. For the test using the blend, differential pressure started to increase 61 hours after the fluid temperature reaches 32 ^{c}F. A complete plug formed 22 hours after the initial increase of differential pressure. The test using OK Sweet crude oil shows an initial increase of differential pressure 76 hours after the fluid temperature reaches 32 ^{o}F. After differential pressure started to increase, it only took 4 hours to reach a complete plug.

The time required for initial differential pressure increase and final complete plug may be related to the test fluid properties. The densities of the three test fluids are close, but the viscosities vary a lot. Fluid viscosity has effect on the emulsion stability. Water droplets and ice particles may be well entrained in the fluid with high viscosity. Since fluid densities are close and flow rate remains the same, viscosity determines Reynolds number. Reynolds number for the tests using kerosene is about 15000 at 26 ^{o}F, indicating the flow pattern is turbulent flow. Water droplets and ice particles may be well dispersed under turbulent flow conditions. Reynolds numbers for the blend tests and OK-Sweet tests are 2100 and 250 at 26 ^{o}F, respectively. The flow condition is laminar flow. In addition, wax exists in the blend and the OK Sweet crude oil. Wax deposition occurred before water freezes, and thus may have effect on ice deposition.

The observed ice accretion in front of the plate looked like “caviar”. The measured water contents of the caviar were in the range between 20% to 40%. After the initial accumulation, the perforated plate, behaving as a filtration equipment, consolidated the caviar by filtrating out the free liquid (test fluid) from the accumulation. [14] During the filtration process, the differential pressure increased as the permeability decreased. A filter cake upstream of the perforated plate formed. The lengths of the filter cake of all the experiments were measured, with the range between 1.1 inch to 1.4 inches.

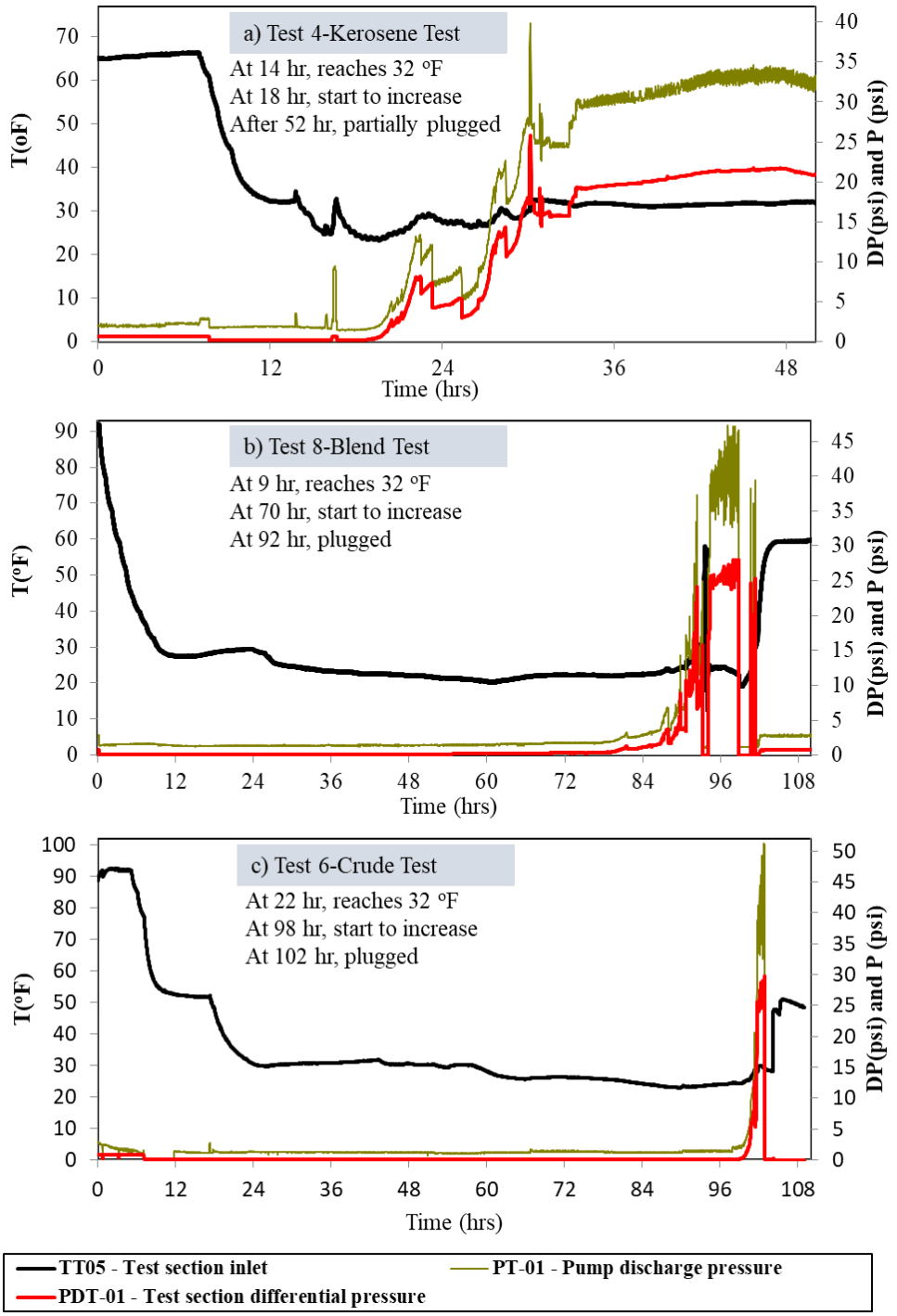

Figure 6: Experimental data comparison for Kerosene Test, Blend Test and Crude Test

The effect of water cut was performed using the blend of kerosene and OK Sweet, which was shown in Figure 7. In Test 7 (Initial WC=1.9%), differential pressure started to increase 32 hours after fluid temperature reaches 32 °F. A complete plug formed 17 hours after the initial increase of differential pressure. In Test 11 (Initial WC=0.8%), differential pressure started to increase 35 hours after fluid temperature reaches 32 °F. A complete plug was not observed during the test.

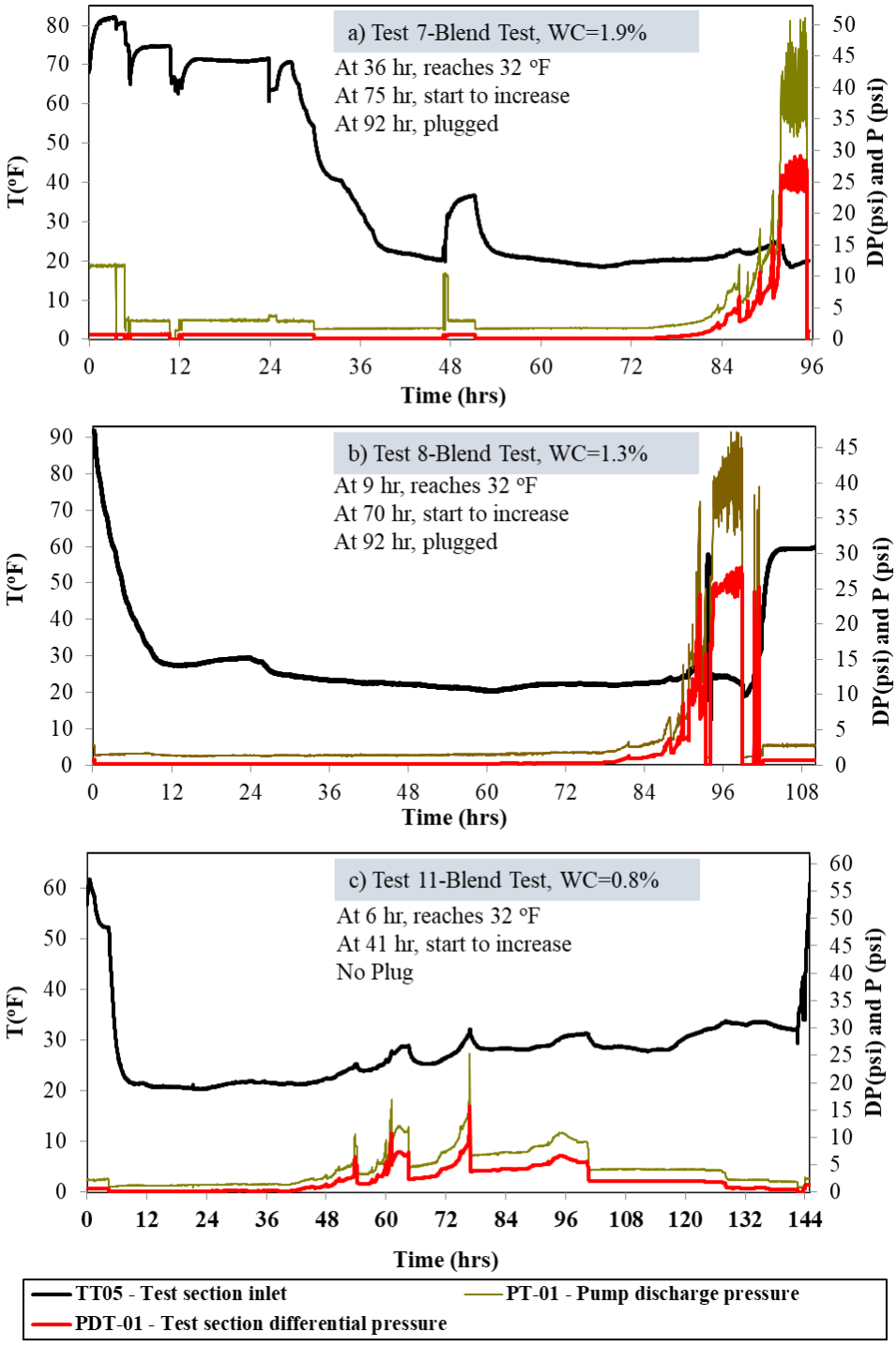

Figure 7: Experimental data comparison for Kerosene Test, Blend Test and Crude Test

Deposition on Pipe Surface

Deposition layers were found in all of the experiments. In addition to ice, wax was also found in the deposition layer for the tests using the OK Sweet and the blend.

Figure 8 shows the ice deposition in the second cooling section in Test 4, which used kerosene as the test fluid. The pictures were taken after the test fluid were drained. Figure 8 a) shows ice deposition along the pipe in the second cooling section, Figure 8 b) and c) show ice deposition before the plate and after the plate in the test section. Figure 8 d) shows that ice deposition in the second cooling section was pigged out for analysis. The water cut of the deposition is 20.1%, while the initial water cut of Test 4 is 1.4%, which indicates ice can deposit and accumulate along the pipe wall. However, the fact that the deposition layer only have 20.1% of ice implies that the deposition layer is porous with kerosene filling the pores. The morphology of the deposition is rime ice or caviar, which forms due to small ice particles sticking on the pipe surface. The ice grain size in Figure 8 d) is between 0.1 and 0.3 mm.

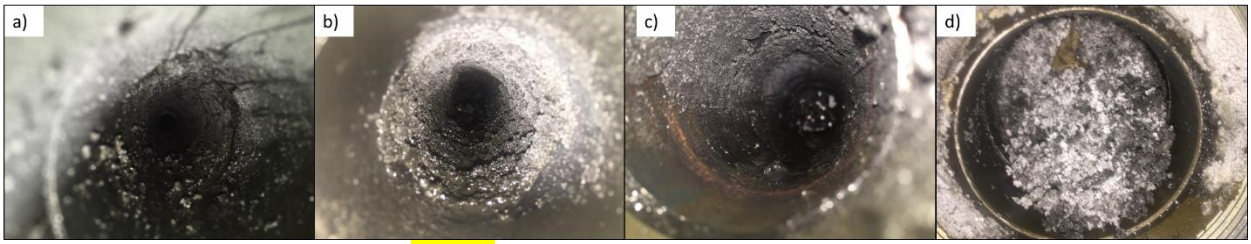

Figure 8: Ice deposition in Test 4

Figure 9 shows the deposition layer for Test 7, which used the blend. The deposition layer was made of ice and wax mixture. Figure 9 a) and b) show the deposition before and after the plate in the test section. The water cut of deposition layer is 21.2%, while the initial water cut is 1.9%. The wax content of the deposition is 1.8%, while the wax content of the blend is 1.4%. The deposition layer is also porous. The deposition layer looks like rime-ice or caviar. Ice particles sticking to the pipe surface leads to this morphology. It is difficult to tell the mechanism of wax deposition on the pipe surface, e.g. molecular diffusion or particle sticking. [15]

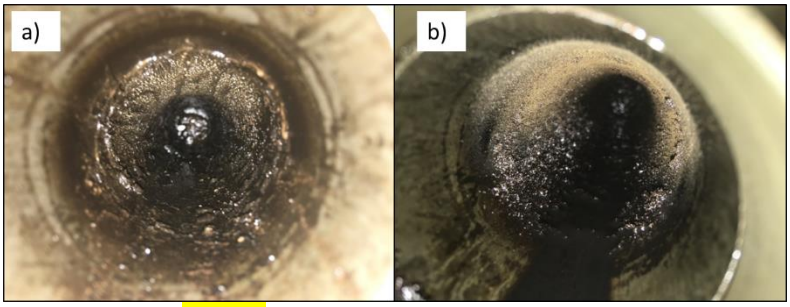

Figure 9: Ice deposition in Test 7

In addition, ice deposition layer was found only at places where a negative temperature gradient existed. Figure 10 shows examples of the ice deposition in the kerosene tests. Figure 10 a) shows the ice deposition layer after the thermocouple TT-04, where the pipe was jacketed and cooled by coolant. Before TT -04, no ice deposition was found. Figure 10 b) and c) show the area near TT-05, where the pipe was not jacketed. In Figure 10 b), although an ice plug was found at the thermocouple, a gap existed between the plug and pipe surface. No ice deposition was found on the pipe surface which was not jacketed.

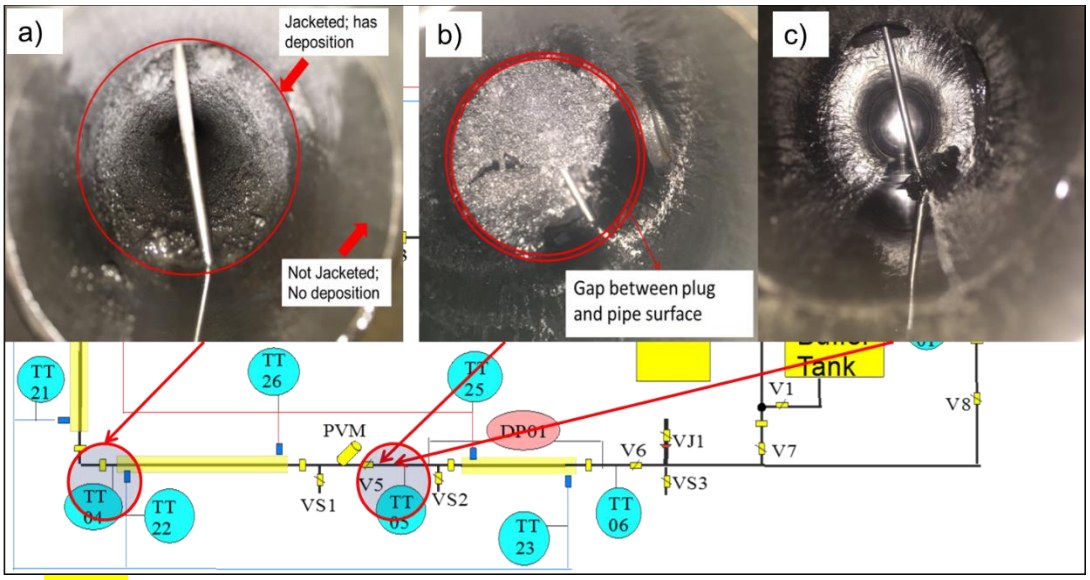

Figure 10: Temperature gradient is required for ice deposition on pipe surface

Deposition and Plugging Evolution throughout Test 10

In Test 10, the test section was disassembled four times to observe the ice deposition and plugging processes during the experiment. The pictures of the deposition along the pipe and the plugging situation on the plate are shown in Figure 11.

After the test section was taken apart for the first time, an annular ice-wax deposition layer was observed. The top of the annular deposition was thinner. A bed was observed at the bottom of the pipe. Behind the plate, the deposition layer was barely there. Ice bedding was observed both before and after the plate. Only two top pores on the plate were open.

After the test section was taken apart for the second time, the annular deposition layers before and after the plate became thicker. Front and back of the plate were covered by ice. The middle right pore and the bottom two pores were plugged.

After the test section was taken apart for the third time, the bottom part of the annular deposition disappeared. The deposition layers were thicker. Only the bottom left pore was plugged.

After the test section was taken apart for the fourth time, the deposition layer became even thicker. The deposition layer after the plate was uniform. The middle and the middle right pores were plugged.

From the evolution of the deposition layer on the pipe surface, we can conclude that the formation of the deposition layer is due to small particles sticking to the pipe surface, which makes the layer become gradually thicker with time. The plugging of plate pores and the deposition on the plate were dynamic processes. Some pores, which were plugged initially, were cleared by flow. Some pores may be plugged again.

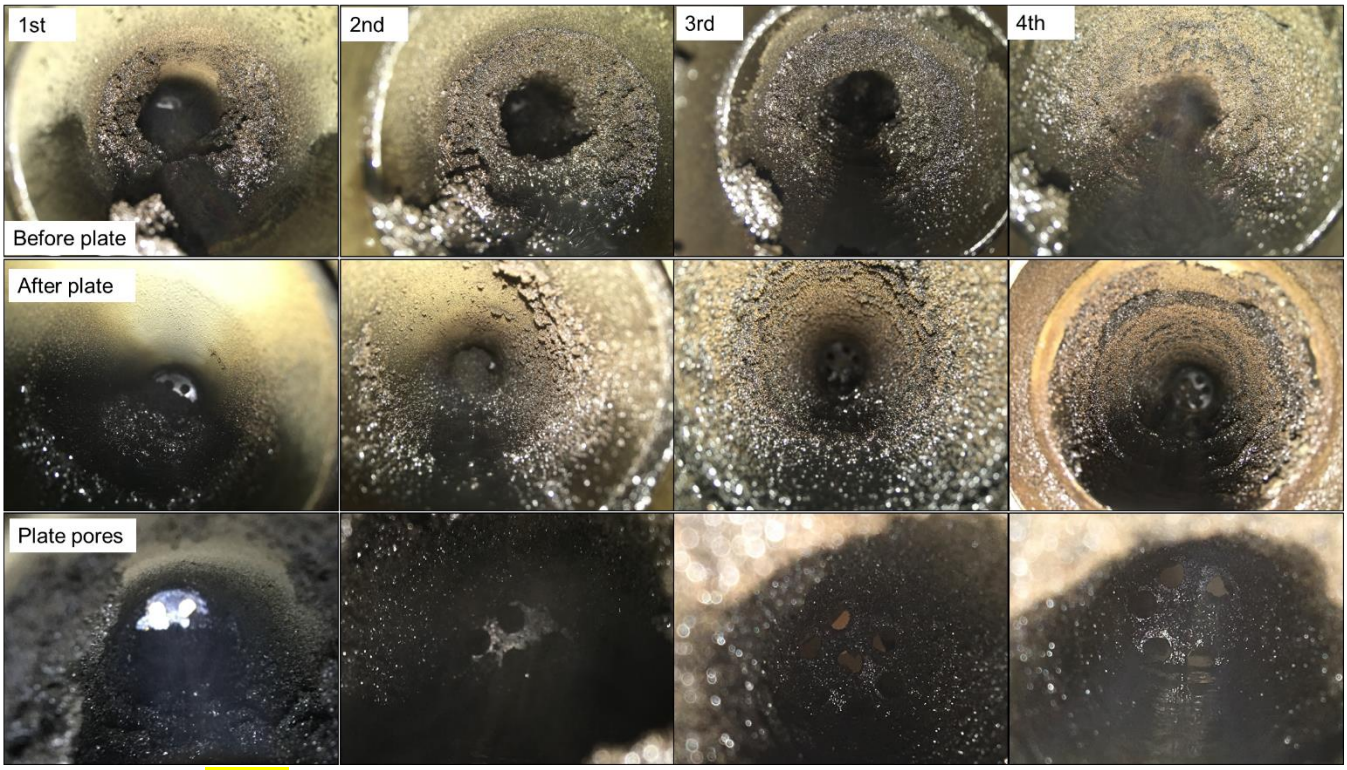

Figure 11: Deposition and plugging evolution throughout Test 10

Mechanisms for Ice Deposition

Based on the experimental results and observations, the following mechanisms for deposition are proposed.

Kerosene Test

Since no wax exists in kerosene, the deposition layer consisted of ice. Figure 12 shows the proposed process for ice deposition in kerosene tests. At the beginning, although the dissolution of water in kerosene is low, an initial ice deposition layer can form due to molecular diffusion or Soret diffusion. Then, larger ice particles stick to the initial layer due to Brownian diffusion or gravitational settling. In this process, larger particles form due to particle interaction and sloughing. Both deposition and sloughing occur. The convex part along the deposition layer is sloughed off. In the end, the deposition layer became smoother.

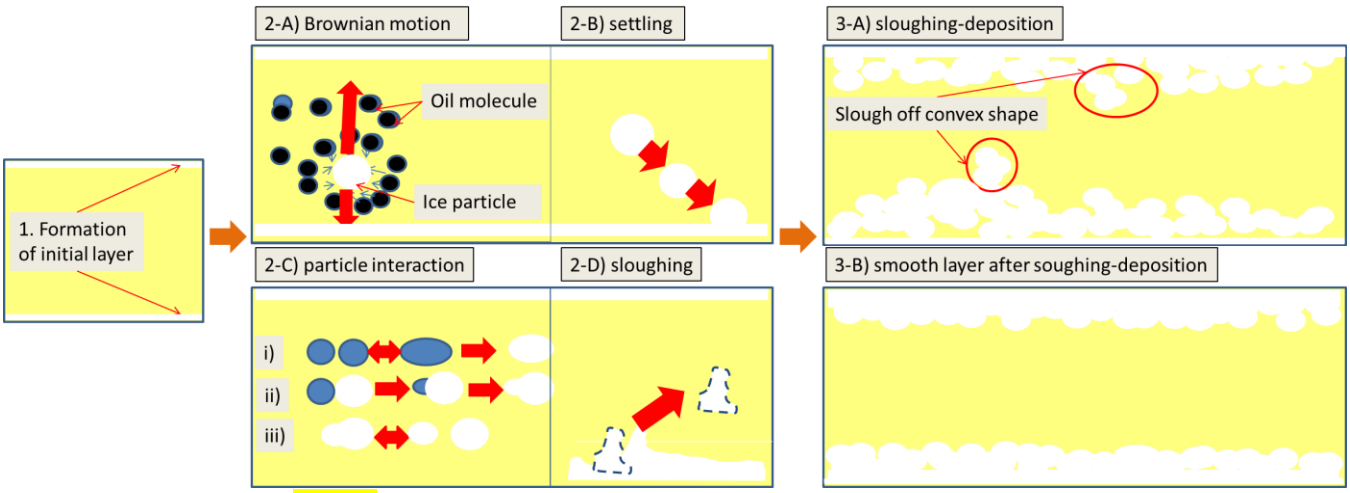

Figure 12: Deposition mechanism for kerosene tests

Crude Oil Test

Since wax appearance temperature was higher than the freezing point of water, wax precipitation and deposition occurred before water froze. Thus, the deposition layer in the crude oil tests is composed of wax and ice. The formed wax deposition layer is porous, which enables water droplets to fill in the pores. After water in the deposition layer freezes, an ice-wax layer will form. In addition, Brownian motion, particle interaction, and sloughing-deposition process also occur in the crude oil tests.

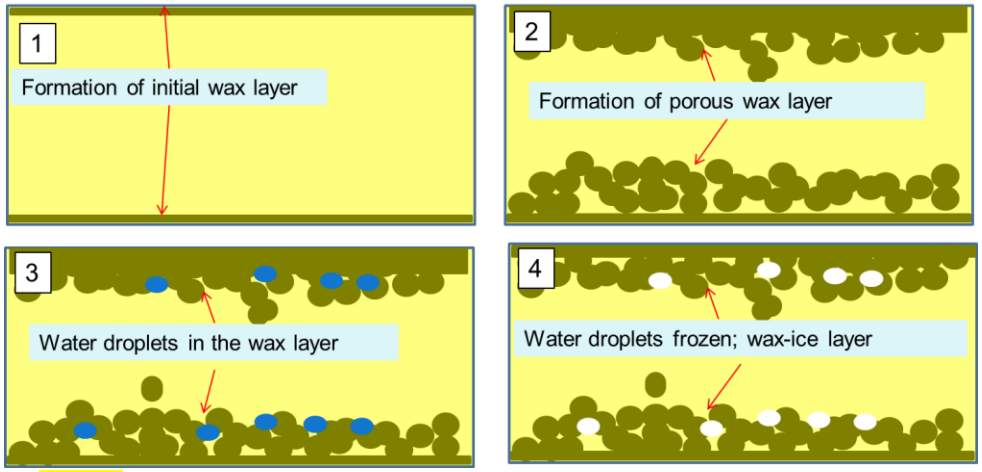

Figure 13: Formation of wax deposition and its effect on ice formation

Mechanisms for Ice Plugging

Plugging mechanisms at the low spot, the inserted thermocouple, and the perforated plate are proposed. At the low spot, ice particles need to climb up to pass through the flow meter. Some of the ice particles settle and accumulate at the low spot, which cause a plug to form.
Two mechanisms are proposed to explain the plug at the inserted thermocouple. When a large ice particle tries to pass through the inserted thermocouple, the ice particle can be broken by the

thermocouple, leaving a residue on the thermocouple for further ice deposition to grow based on the residue. In addition, if large ice particles stuck on the thermocouple, the accumulation of the ice particles will restrict flow.

The plugging at their thermocouple is due to the formation of large particles or the deposition layer. If particles become large enough, the pore can be plugged by the particles. The size of particle to plug the plate pores is not large enough to be blocked by the thermocouple. Thus, if the plate was plugged, no plugging was found at the thermocouple.

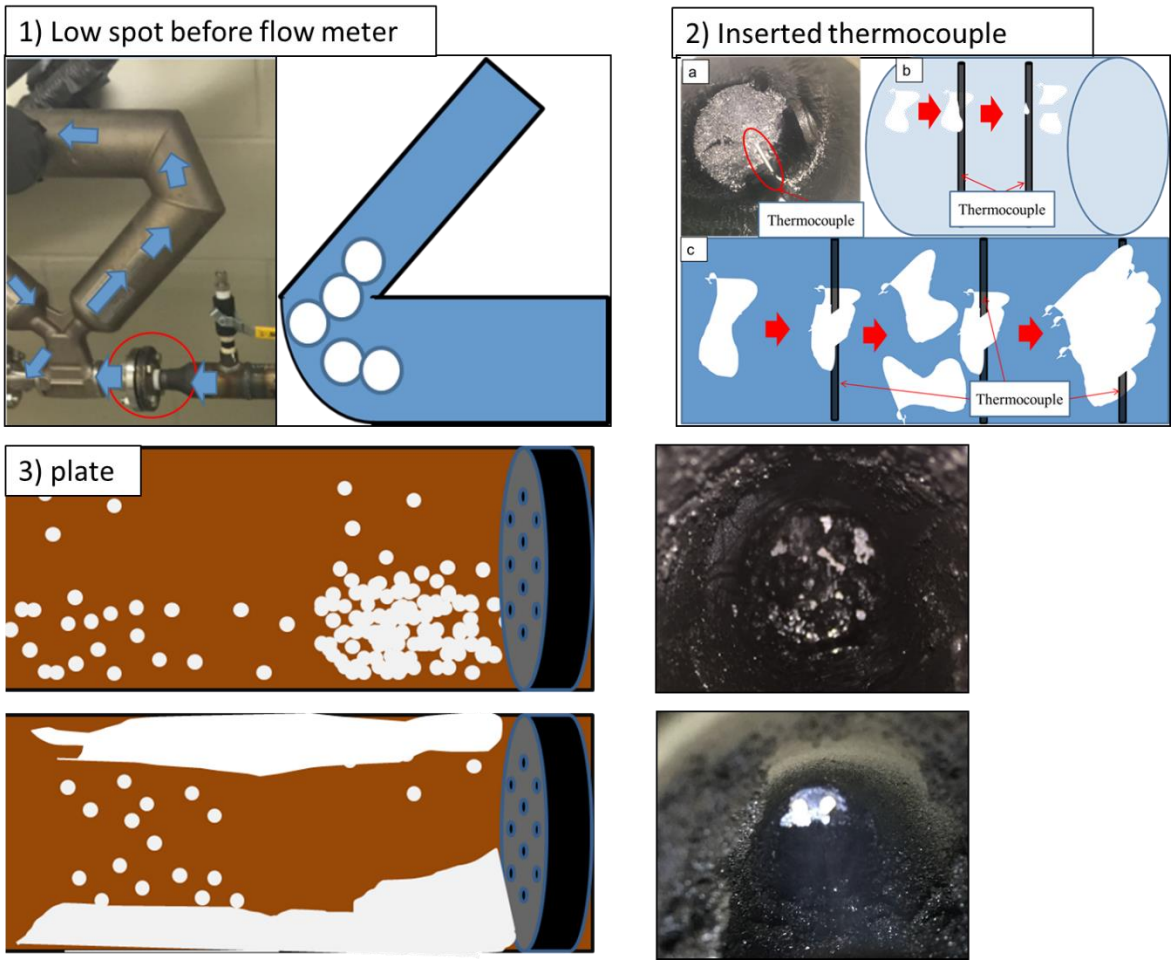

Figure 13: Plugging mechanisms at the low spot, the thermal couple, the and plate

Conclusions

Experiments on ice formation in a flow loop have been carried out. Restriction of flow due to ice formation was found at the low spot, the inserted thermocouple, and the perforated plate. Annular deposition layer was identified at locations where a negative temperature gradient exists. Experimental results also suggest that if the working fluid is more viscous and the water cut is smaller, longer wait time is required before P and DP starts to increase. In addition, if the fluid is more viscous and more water exists in the fluid, less time is required for a final plug to form. The evolution of deposition and plugging was observed. Ice deposition and plugging mechanisms are

proposed.

Acknowledgements

The authors would like to thank the Alyeska Pipeline Service Company for supporting this research project. The authors would also like to thank Dr. Yaqin Wu and Marc Tappert at ConocoPhillips for measuring properties of fluids used in this project.

Reference

1. Sunne, S., *Ice may delay restart of pipeline's breached Montana section*. Reuters. Retrieved from http://www.reuters.com/article/us-bridgerpipeline-oilspill-idUSKBN0KS1VE20150120
2. APSC, A. P. S. (2011). *Low Flow Impact Study-FINAL REPORT*. Alyeska Pipeline Service Company
3. Bird, K., Charpentier, R., Gautier, D., Houseknecht, D., Klett, T., Pitman, J., Moore, T., Schenk, C., Tennyson, M., and Wandrey, C., *Circum-Arctic Resource Appraisal: Estimates of Undiscovered Oil and Gas North of the Arctic Circle*. U.S. Geological Survey, USGS Fact Sheet
4. Dendy, S., *Natural Gas Hydrates in Flow Assurance*. Gulf Professional Publishing, 2010.
5. Sinquin, A., Palermo, T., Peysson, Y., *Rheological and flow properties of gas hydrate suspension*s. Oil Gas Sci. Technol. 2004, 59 (1), 41−57.
6. Frostman, L. M., *Anti-agglomerant hydrate inhibitors for prevention of hydrate plugs in deepwater systems*. Proceeding of the SPE Annual Technical Conference and Exhibition; Dallas, TX, Oct 1−4, 2000
7. Gudmundsson, J. S., *Cold flow hydrate technology.* Proceeding of the 4th International Conference on Gas Hydrates. Yokohama, Japan, May 19−23, 2002.
8. Turner, D. J., Talley, L., *Hydrate inhibition via cold flow - No chemicals or insulation.* Proceeding of the 6th International Conference on Gas Hydrate; Vancouver, British Columbia, Canada, July 6−10, 2008.
9. Rosenfeld, D., Woodley, W. L., *Deep convective clouds with sustained supercooled liquid water down to-37.5 degrees C*. Nature, 405(6785), 440.
10. Myers, T.G. and Charpin, J.P., *A mathematical model for atmospheric ice accretion and water flow on a cold surface*. International Journal of Heat and Mass Transfer, *47*(25), 5483-5500.
11. Kitanovski, A. and Poredoš, A., *Concentration distribution and viscosity of ice-slurry in heterogeneous flow*. International Journal of Refrigeration, 25(6), 827-835.
12. Lafond, P.G., 2014. *Particle jamming during the discharge of fluid-driven granular flow* (Doctoral dissertation, Colorado School of Mines. Arthur Lakes Library).
13. Xu, H., E. Pereyra, E. Dellacase, and M. Volk., *Study on Ice Formation and Its Effect in Oil Pipelines*. Proceeding of ofn Arctic Technology Conference. Offshore Technology Conference, 2016.
14. Xu, H, *Hydrate desalination using cyclopentane hydrates*. Colorado School of Mines, 2013.
15. Chi, Y., Daraboina, N. and Sarica, C., *Effect of the Flow Field on the Wax Deposition and Performance of Wax Inhibitors: Cold Finger and Flow Loop Testing.* Energy & Fuels, 31(5), 4915-4924.